The Features of Ozone Quasi-Biennial Oscillation in Tropical Stratosphere and Its Numerical Simulation

Chen Yuejuan (陈月娟)[1], Zheng Bin (郑 彬), and Zhang Hong (张 弘)

Department of Earth and Space Sciences, University of Science and Technology of China, Hefei, 230026

(Received June 22, 2001; revised May 8, 2002)

ABSTRACT

The interannual variation of the vertical distribution of ozone in the tropical stratosphere and its quasi-biennial oscillation (QBO) is analyzed using HALOE data. The results are compared with the wind QBO. A numerical experiment is carried out to study the effects of wind QBO on the distribution, and variation of ozone in the stratosphere by using the NCAR interactive chemical, dynamical, and radiative two-dimensional model (SOCRATES). Data analysis shows that the location of the maximum ozone mixing ratio in the stratosphere changes in the meridional and vertical directions, and assumes a quasi-biennial period. The meridional and vertical motion of the maximum mixing ratio leads to a QBO of column ozone and its hemispheric asymmetry. The QBO of the location of the maximum is closely connected with the zonal wind QBO. The data analysis also shows that in the tropical region, the phase of the QBO for ozone density changes many times with height. Numerical simulation shows that the meridional circulation induced by the wind QBO includes three pairs of cells in the stratosphere, which have hemispheric symmetry. The transport of ozone by the induced meridional circulation in various latitudes and heights is the main dynamic cause for the ozone QBO. Cells of the induced circulation in the middle stratosphere (25–35 km) play an important role in producing the ozone QBO.

Key words: ozone quasi-biennial oscillation (QBO), HALOE data, NCAR model, numerical simulation, SOCRATES

1. Introduction

Many studies have been done on the interannual variation of ozone amount and the quasi-biennial oscillation of ozone (QBO). For example, Funk and Garnham (1962) and Ramanathan (1963) first discovered the QBO of ozone and its relation to the QBO of upper winds at low latitude by analyzing the total ozone amount over the tropics. Further studies show that the ozone QBO also exists over the extratropics but with a phase reversal compared with that in the tropics, and the phases reverse near 12° latitude with hemispheric asymmetry (Hasebe 1983; Yang and Tung 1995); the phase of ozone QBO in the lower stratosphere is always opposite to that in the upper stratosphere (Hasebe 1994). The results from observational data have been confirmed by numerical simulations carried out by Gray and Ruth (1993) and Hess and O'Sullivan (1995). Jones et al. (1998) simulated the transport of stratospheric trace gases by zonal wind QBO, and pointed out that the wind QBO would induce a meridional circulation that transports long-lived traces from the tropics to the extratropics and would produce a QBO in the extratropics. In recent years, the related research has been taken up in China. Analyzing the TOMS data from 1980 through 1987, Li et al. (1997) found that the

[1]E-mail: cyj@ustc.edu.cn

strength of ozone QBO signals in the Northern Hemisphere is generally larger than in the Southern Hemisphere and that the intensity distribution appears to have hemispheric asymmetry. Chen and Huang (1996) used the 34-level coupled planetary wave—zonal flow spectrum model to study the effects of planetary wave transport on ozone in the mesosphere. At the same time, the influences on ozone transport by zonal wind QBO over the tropics were studied, and they found that the difference between ozone transport over the tropics and extratropics is due to the difference of the secondary meridional circulation forced by the easterly and westerly shear over the tropics, while the difference in the middle and high latitudes is due to the different ozone transport by planetary waves at different phases of tropical zonal wind QBO. Zhang et al. (2000) used the NCAR interactive chemical, radiative, and dynamical two-dimensional model to study the influences of the zonal wind QBO on the distribution of stratospheric tracers, and they discussed the induced meridional circulation by wind QBO and its influences on ozone QBO. Gradually, more and more was learned about ozone QBO in these studies. However, for lack of observational data at the time, most of the results were obtained by analyzing the total ozone amount, so the vertical structure of the ozone QBO is unclear. The modeled secondary meridional circulations induced by zonal wind QBO are symmetric about the equator over the tropics and the extratropics, but the ozone QBO produced by the induced circulation is asymmetric. The reasons for this phenomenon are expected to come from further study. In the last decade, more and more satellite data included not only the total amount of ozone but also the three-dimensional distribution of ozone, which provides a good data foundation for studying ozone QBO. Using the HALOE data from 1992 to 2000, we analyze the vertical distribution of the ozone mixing ratio and study the interannual variation of the ozone distribution and the structures of the ozone QBO in the stratosphere. We then compare the ozone QBO with the zonal wind QBO over low latitudes and investigate the relationship between them. At last, we explore the mechanism of ozone QBO generation through simulation using the NCAR interactive chemical, radiative, and dynamical two-dimensional model (SOCRATES).

2. Observational data

The Halogen Occultation Experiment (HALOE) is an instrument on the Upper Air Research Satellite (UARS), which uses the solar occultation approach to observe solar radiation absorbed by tracers and aerosols along the earth limb for one sunrise and one sunset event on every satellite orbit. It retrieves the vertical distribution of the tracers and aerosol extinction efficiency. The vertical distributions of O_3, HCl, HF, CH_4, H_2O, NO, and NO_2, the extinction coefficients of the aerosols and the temperature can be obtained at the same time. The latitude coverage is from 80°S to 80°N with slight seasonal change, and the vertical range is from 5 km to 60–130 km with a vertical resolution of about 500 m in the stratosphere. The instrument has worked since 11 September 1991 and its observational data are in excellent agreement with ATMOS data of 1992.

The HALOE data used in this paper were downloaded from the Internet and consist of sunrise ozone data from January 1992–February 2001 and sunset ozone data from June – August 1997 (due to an absence of sunrise data). UARS is a polar-orbiting satellite so that in various observations, the HALOE provides data for different times and positions, depending on the orbit. For a more convenient comparison, objective analyses are made on the HALOE data and $5° \times 5°$ gridded data are obtained (covering 70°S–70°N, 180°W–180°E).

Zonal wind data comes from NCEP/NCAR data.

3. Results from observational data

The ozone QBO in recent years has been analyzed and discussed by Dunkerton and Timothy (2001) with the HALOE data in the 1992–1999 period. The analysis will not be repeated here. Here we will discuss the seasonal and interannual variation of the vertical distribution of ozone in the stratosphere.

3.1 *Seasonal and interannual variation of vertical distribution of ozone mixing ratio in the stratosphere*

Figure 1 shows the latitude–pressure cross-sections of the zonal mean ozone mixing ratio averaged from 1992 to 2000 by season. It can be seen that the area with high ozone mixing ratio is located between 20 hPa and 4 hPa with the peak value larger than 9 ppmv, which is near 10 hPa in low latitudes and decreasing toward the poles. The location of the high ozone mixing ratio changed with the seasonal variation of solar radiative intensity in various latitudes. It was located north of the equator from June–August (JJA) as shown in Fig. 1b,

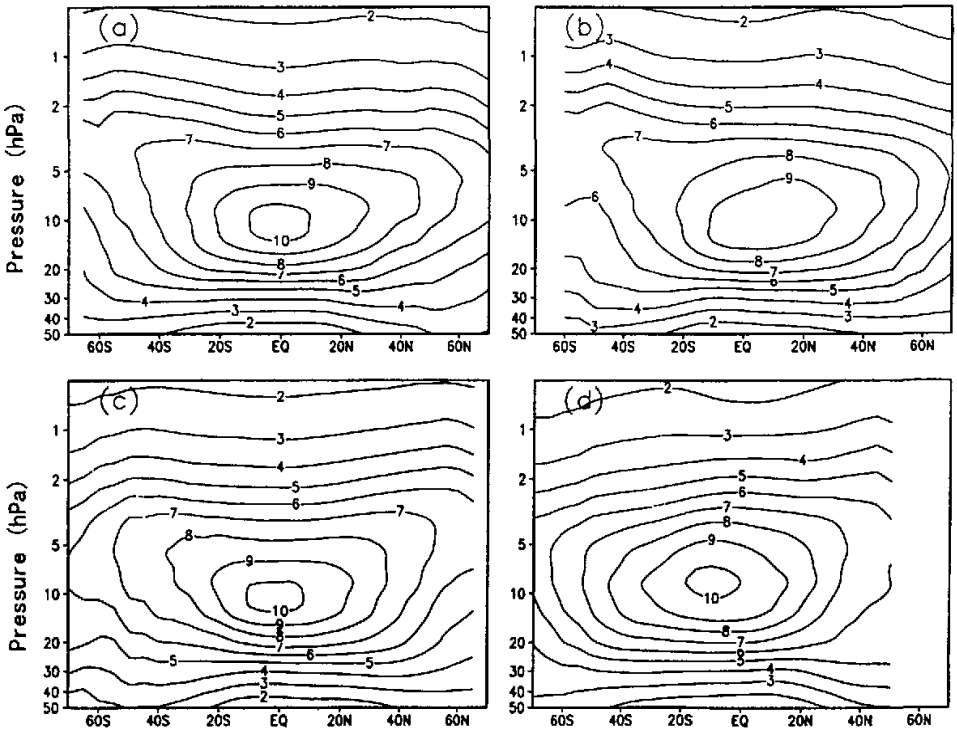

Fig. 1. Latitude–pressure cross section of zonal mean ozone mixing ratio averaged from 1992 to 2000. (a) For MAM, (b) for JJA, (c) for SON, and (d) for DJF. (Blanks in the figure represent an absence of data, similary hereafter). Unit: ppmv

moving south of the equator from December – February (DJF) as shown in Fig. 1d. From March – May (MAM) and September – November (SON) it is approximately over the equator as shown in Figs. 1a and 1c.

Aside from the seasonal variation in the vertical–meridional distribution of the ozone mixing ratio, the interannual variation of the disribution is also noticeable. First, consider the distribution in JJA. Figure 2 shows the latitude–pressure cross section of the zonal mean ozone mixing ratio in JJA for each year. We can see from the figure that the values of ozone density in the center continued to decrease year by year from 1992 to 1995. The values changed little in 1996 and 1998, and increased somewhat in 1999 and 2000. Figure 2 also shows that the locations of high ozone mixing ratio changed from year to year. The maximum region in 1992 is located to the north with the center near 12°N, and in 1993, the maximum region moved southward, and its center moved to 3°N. The maximum moved northward to 15°N in 1994 and went back to 1°N in 1995. In the same way, the maximum moved northward in 1996, 1998, and 2000, and moved near the equator in 1997 and 1999. These motions of the high mixing ratio in the north / south direction occurred in JJA, clearly showing the QBO signal.

According to the NCEP data, the averaged zonal winds at 80–10 hPa over the equator are easterly in 1992, 1994, and 1996 and westerly in 1995 and 1997. In 1993 the wind changed from westerly to easterly. Comparing with the motion of the maximum ozone mxing ratio, we

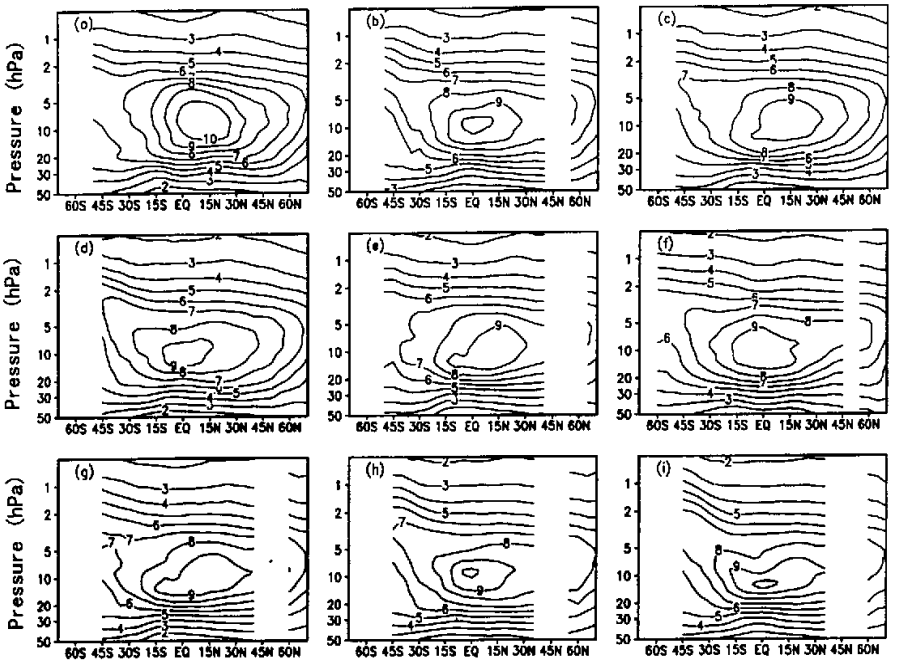

Fig. 2. Latitude–pressure cross section of zonal mean ozone mixing ratio in JJA for (a) 1992, (b) 1993, (c) 1994, (d) 1995, (e) 1996, (f) 1997, (g) 1998, (h) 1999, and (i) 2000. Unit: ppmv

can see the relationship between zonal wind QBO and the QBO of the maximum ozone mixing ratio. In JJA, the westerly at 80–10 hPa over the equator corresponds with the center location moving towards the equator, while the easterly corresponds to the center moving northward.

In DJF, the QBO signals follow the same pattern except that the maxima are located mainly in the Southern Hemisphere. Furthermore, when it moved in the north / south direction, the maximum region also moved vertically accompanied by a change in thickness. When it expanded upward (downward), its thickness increased (decreased). The increment (decrement) can be 1–2 hPa which is about 10%–20% of the average thickness of the area of maximum ozone mixing ratio.

Table 1. *The meridional and vertical limits and center location of the region of high ozone mixing ratio (>9 ppm), and the zonal wind direction in MAM*

Year	Meridional limits	Vertical limits (hPa)	Center location (hPa)	Zonal wind
1993	20°S–29°N	15–6	9	W
1994	24°S–32°N	17–9	13	E
1995	25°S–20°N	15–5	9	W
1996	23°S–30°N	16.5–8	11	E
1997	25°S–14°N	15.5–5	9	W
1998	21°S–25°N	16–5	10	E
1999	20°S–23°N	16–6	9	
2000	23°S–34°N	16–7	11	

In MAM, the region of high ozone mixing ratio in all years was nearly over the equator; the changes in the region were mainly motion in the vertical direction and the variation of its thickness. When the high region moved downward and became thinner, it spread southward and northward. Table 1 gives the meridional and vertical limits of the region of ozone mixing ratio higher than 9 ppm, the location of its center, and the zonal wind direction in MAM for every year. The table shows the quasi–biennial oscillation of the location and thickness of the high region of ozone mixing ratio and its relation to the wind QBO. When the zonal winds over the equator formed a westerly, the high region spread upward and thickened. In this case, the column ozone amount increased over the equator and decreased over the extratropics. While in the case of an easterly, the location of the high region was lower and it was thinner, the column ozone amount decreased over the equator and increased over the extratropics. The situation in SON is similar to that in MAM.

3.2 *The vertical structure of ozone QBO in stratosphere*

In order to clearly see the vertical structure of ozone QBO, we analyzed the variation of the vertical distribution of the zonal mean departure of ozone mixing ratio. Figure 3 shows the height–time series of the departure over the equator. It is clear that the phase of ozone QBO changed many times with height over the equator. The phase of ozone QBO at the 50–20 hPa level was opposite to that near 13 hPa, while alike near 5 hPa. At about the 2–3 hPa level, the phase changed again, however the features of the QBO at this level are not as clear as those in the lower levels. The vertical structure of ozone QBO over the equator is more complex than the results obtained by Hasebe (1994), pointed out that the phase of

ozone QBO in the lower stratosphere is always opposite to that in the upper stratosphere. The wind phases marked at the bottom of Fig. 3 are the zonal wind phase at 20 hPa over the equator. We can see the relationship between the phase change of wind QBO and ozone QBO.

The vertical structure of ozone QBO over 30°N and 30°S are not the same as that over the equator. Specifically, the phase of ozone QBO over 30°N from 50 hPa to 5 hPa does not change very much, and is opposite to the phase over the equator from 50 hPa to 20 hPa. Also the phases above 5 hPa over 30°N are opposite to those below 5 hPa (figures omitted).

4. Model used in the numerical simulation

The NCAR two-dimensional model named SOCRATES, is used in the simulation of chemistry, radiation, and dynamical transport of environmentally important species (Huang et al. 1997). Its dynamical equations include the equation of heat flux, equation of momentum, equation of continuity, and thermal wind with eddy heat flux diffusion, planetary wave, gravity wave, and tidal wave forcing. The forcing and diffusion are functions of zonal wind and can be solved based on the theory of linear waves. Though the wave forcing is parameterized in the model, the waves can respond and interact with the mean flow.

In the radiative part of the model, the net diabatic heating rate consists of the solar

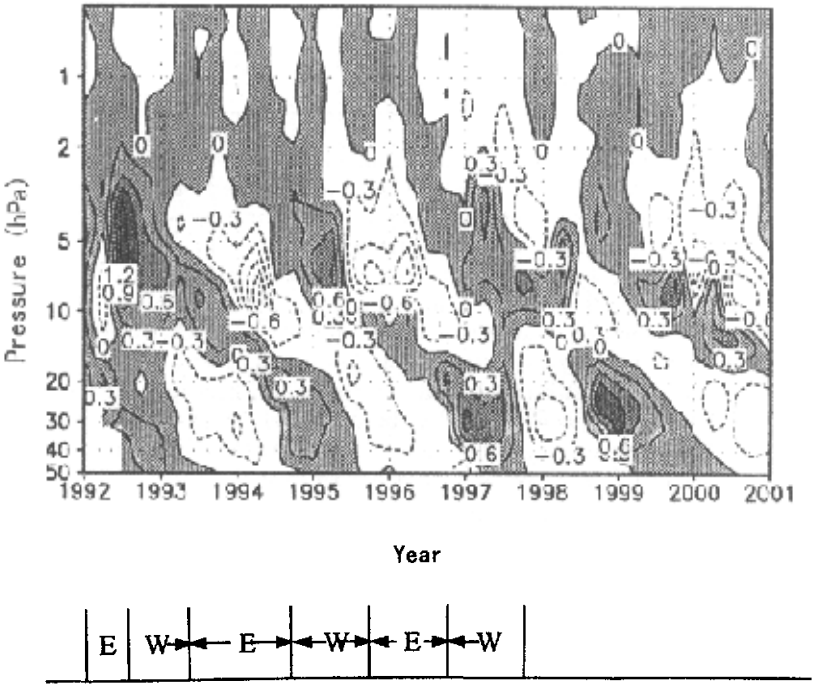

Fig. 3. Height-time series of the zonal mean departure of ozone mixing ratio over the equator. Units: ppmv. The zonal wind phase at 20 hPa is marked at the bottom of the figure.

heating rate (Q_S) and infrared cooling rate (Q_{IR}), calculated according to the method of NCAR CCM1.

The chemical part of the model is composed of 74 kinds of chemical species and more than 130 chemical reactions. The chemical species are grouped into three categories: long-lived species and chemical family, intermediate lifetime species, and short-lived species. Since the sensitivities of various lifetime species to the chemical and dynamical process are different, various equations of continuity— transport are adopted. Additonally, polar stratospheric heterogeneous chemistry and aerosol chemistry can be added to the model as options.

The vertical range is from the ground surface to 120 km with a vertical resolution of 1 km. Horizontal coverage is from 85°S to 85°N. The grid length is 5°.

In this experiment, since it is not explicit to resolve the zonal component equation of momentum in the two-dimension model, wind QBO forcing is added into the equation of momentum using the parameterized method, and then temperature QBO and relevant circulation are simulated. The formula for wind QBO forcing is

$$\bar{u}_{QBO} = -\bar{u}_{max}\exp\left[-\left(\frac{\varphi}{\varphi_w}\right)^2\right]\cos\left(\frac{\pi}{2}\cdot\frac{\varphi}{\varphi_w}\right)\cos\left(\frac{z-z_{max}}{h_{QBO}}\pi\right)\cdot\cos\left(2\pi\frac{t-1}{t_{QBO}}+2\pi\frac{z-z_{max}}{z_{hfwd}}\right),$$

where $\bar{u}_{max} = 25\ m\ s^{-1}$, is the maximum amplitude of the wind QBO, the QBO disturbance is taken as a Gaussian function of latitude, $\varphi_w = 15°$ is the Gaussian width, the disturbance follows a sine-shaped change with height, the maximum disturbance appears at $z_{max} = 28$ km, the half width $z_{hfwd} = 27$ km, h_{QBO} is the vertical limits of the wind QBO which is taken as 24 km, t is the day of integration, and t_{QBO} is the period of wind QBO, taken as 821 days (about 27 months).

The model can calculate not only the transport of ozone and trace gases by the wind QBO, but also the radiation and chemistry due to changes of ozone and tracer density in the stratosphere. The description of this model and the simulated distribution of the trace gases (include ozone) can be found on the NCAR web site. Their simulations agree well with observation. Zhang et al. (2000) used this model to study the effects of wind QBO on tracer distribution in the stratosphere. The results show that in the case where aerosol heterogeneous chemistry and wind QBO are not added to the model, the simulated wind and temperature demonstrate normal seasonal variation, and the simulated distribution of trace gases (such as O_3, HCl, CH_4, N_2O and so on) in stratosphere are consistent with that from HALOE data. When wind QBO is added, the quasi-biennial oscillation of the trace gases is also well simulated. Here we build on this previous work to pursue further results regarding ozone.

5. The simulated results and comparison with the observation

5.1 *The vertical-meridional distribution of ozone mixing ratio in various phases of wind QBO*

Figure 4 gives the simulated latitude-altitude cross-section of ozone mixing ratio for DJF, MAM, and JJA. It can be seen from Figs. 2–4 that the simulated vertical-meridional distributions of ozone mixing ratio in the stratosphere are consistent with HALOE data.

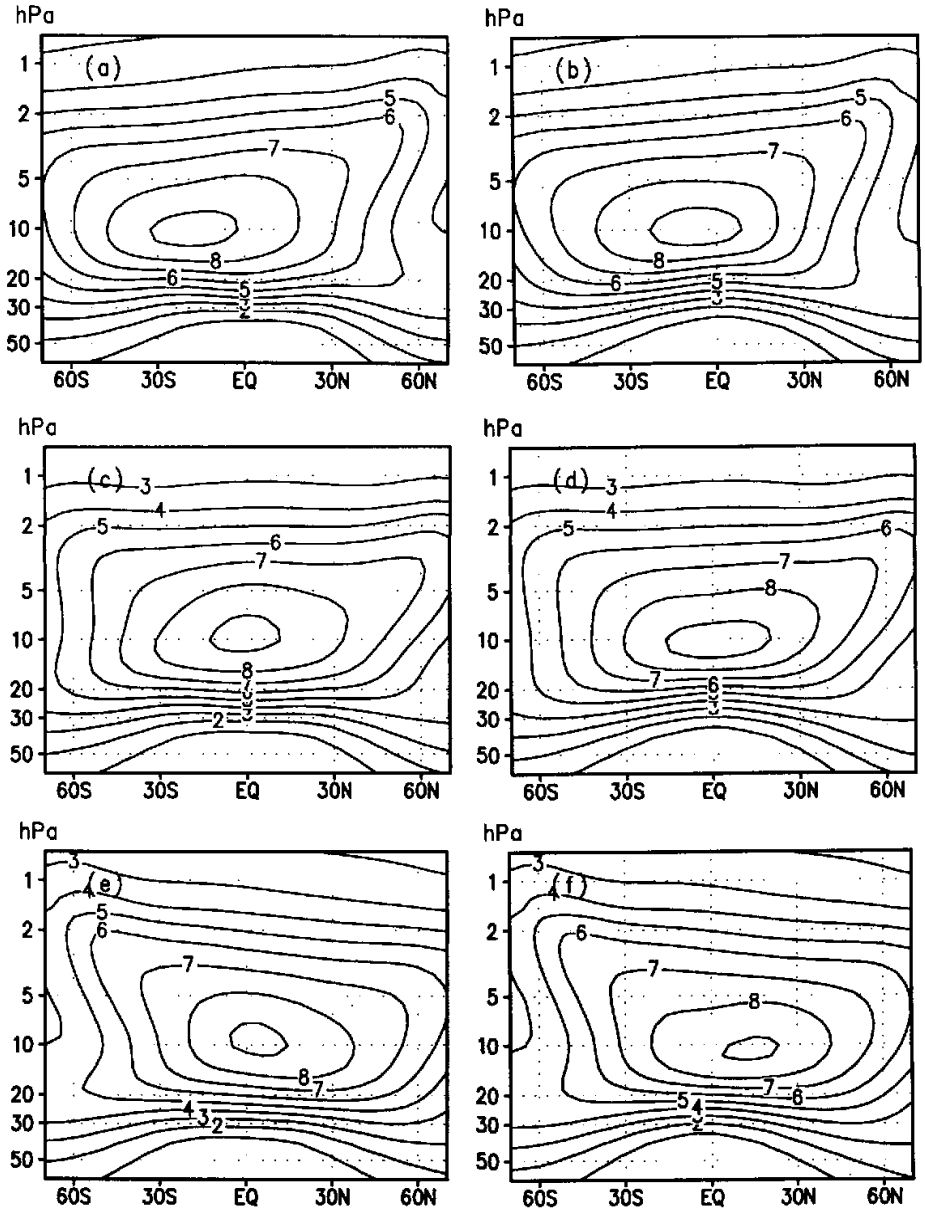

Fig. 4. Simulated latitude–altitude cross section of ozone mixing ratio (in ppmv) using the NCAR two-dimensional model. (a) For DJF in westerly phase, (b) for DJF in easterly phase, (c) for MAM in westerly phase, (d) for MAM in easterly phase, (e) for JJA in westerly phase, and (f) for JJA in easterly phase.

We can also see the QBO signals of the position of maximum ozone mixing ratio from the simulation. The simulated maximum moves in the north–south direction apparently in DJF and JJA (as shown in Figs. 4a, b and Figs. 4e, f). The maximum is located near the equator in the westerly phase of DJF and JJA, while in the easterly phase, it moved near 16°S in DJF and near 16°N in JJA. The simulated position of maximum ozone mixing ratio in MAM was located near the equator, which moved vertically as it changed thickness (as in Figs. 4c, d). When the maximum expanded upward in the westerly phase, its thickness increased and when it went down in the easterly phase, its thickness decreased. The difference in the height of the 8 ppm contour over equator can be more than 1 km. The agreement of the simulation with the HALOE data analysis proved that the QBO of the high region of ozone mixing ratio in the stratosphere is connected closely with wind QBO.

5.2 *The vertical structure of ozone QBO in various phases of wind QBO*

Figures 5 and 6 show the latitude–height cross section of the difference of ozone mixing ratio simulated for the DJF and MAM, and JJA and SON, respectively. Shown is the difference between the simulation with wind QBO and the simulation without wind QBO. From these figures we can see the vertical–meridional structure of ozone QBO in various phases of wind QBO. It is clear that the wind QBO forcing leads to the changing of the phase of ozone QBO many times with height, and it is more clear over equator. The sign of the difference in the easterly phase is opposite to the sign in the westerly phase. The changes of ozone mixing ratio in the extratropics are reverse of those in the tropics, except that the phase reversals occur at lower heights. In addition, we can see changes in the hemispheric asymmetry of the ozone mixing ratio.

It is shown in Figs. 5 and 6 that with an increase in simulation time, the height where the sign reverses descends gradually, and the difference below 20 hPa is less and replaced by the opposite sign of the difference from above gradually. While the simulated value of the difference over 10 hPa increased with it continuously as it moved down. Soon afterwards, a new region with opposite sign appeared at the top. Almost one year passed when the zonal wind changed to another phase, and the phase of ozone QBO changed its reversal with height. Comparing these simulated results with the results from data analysis, we can see that the simulated structures of ozone QBO are in accord with observation. It should be noticed that the difference shown in Figs. 5 and 6 is not due to seasonal variation but the process of the phase change of wind QBO, which will be discussed below.

5.3 *The induced circulation in various phases of wind QBO and its effect on ozone QBO*

In order to give a reasonable explanation for the generation of QBO of the center of high ozone mixing ratio and the vertical structure of ozone QBO, the simulated variations of the meridional circulation induced by wind QBO were analyzed. Figure 7 shows the difference between the meridional circulation simulated with wind QBO forcing and without wind QBO forcing in the westerly phase (we called it residual circulation induced by wind QBO). Figure 8 shows the same thing for the easterly phase. It is analogous to the meridional circulation induced by zonal wind QBO referred to by Jones et al. (1998) and the secondary circulation in the westerly or easterly shear zones over the tropics referred to by Chen and Huang (1996). We can see from Figs. 7 and 8 that the residual circulation consists of three pairs of cells aligned vertically from 120 to 1.5 hPa (about 15–45 km). The three pairs of cells are hemispherically symmetric below 5 hPa.

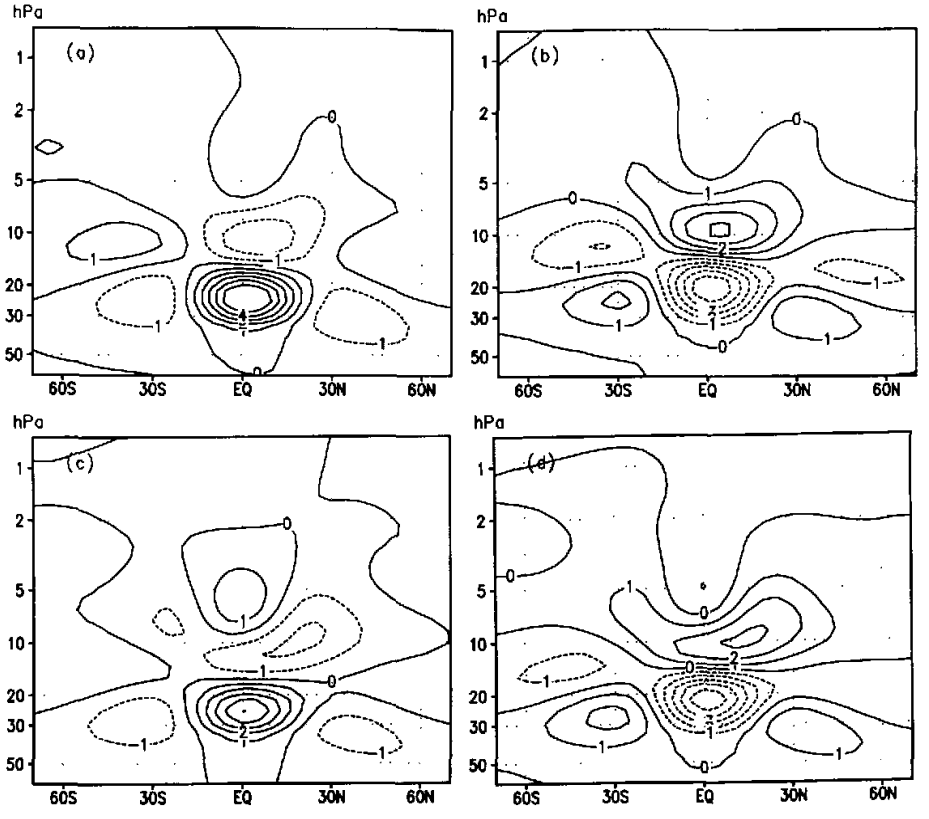

Fig. 5. Simulated latitude–height cross section of the difference of ozone mixing ratio (in ppmv) (values with wind QBO minus the values without wind QBO). (a) For DJF in westerly phase, (b) for DJF in easterly phase, (c) for MAM in westerly phase, and (d) for MAM in easterly phase.

In the October of the first model year (Fig. 7a) when the westerly phase began and started to increase in intensity, the three pairs of cells were located at the levels below 50 hPa, 50–10 hPa, and above 10 hPa, respectively. The cells in the middle were stronger, in which the flow went downward over equator and separated to the south and north at the level near 50 hPa, turning upward in the extratropics and going back to the equator at about 10 hPa. The cells below 50 hPa and above 10 hPa went to the opposite direction, compared with the cells at 50–10 hPa. With an increase in simulation time, the three pairs of cell moved down gradually. In the January of next model year, they moved to the levels below 70 hPa, 70–12 hPa and above 12hPa, respectively. During the movement, the middle cells were weakened and the upper cells strengthened. When the simulation reached July of the second model year, when the westerly phase started to weaken, the middle cells moved to the level below 35 hPa and replaced the lower cells gradually. At the same time, the cells which were originally above moved to 35–5 hPa and new cells appeared above 5 hPa. In October of the second model year

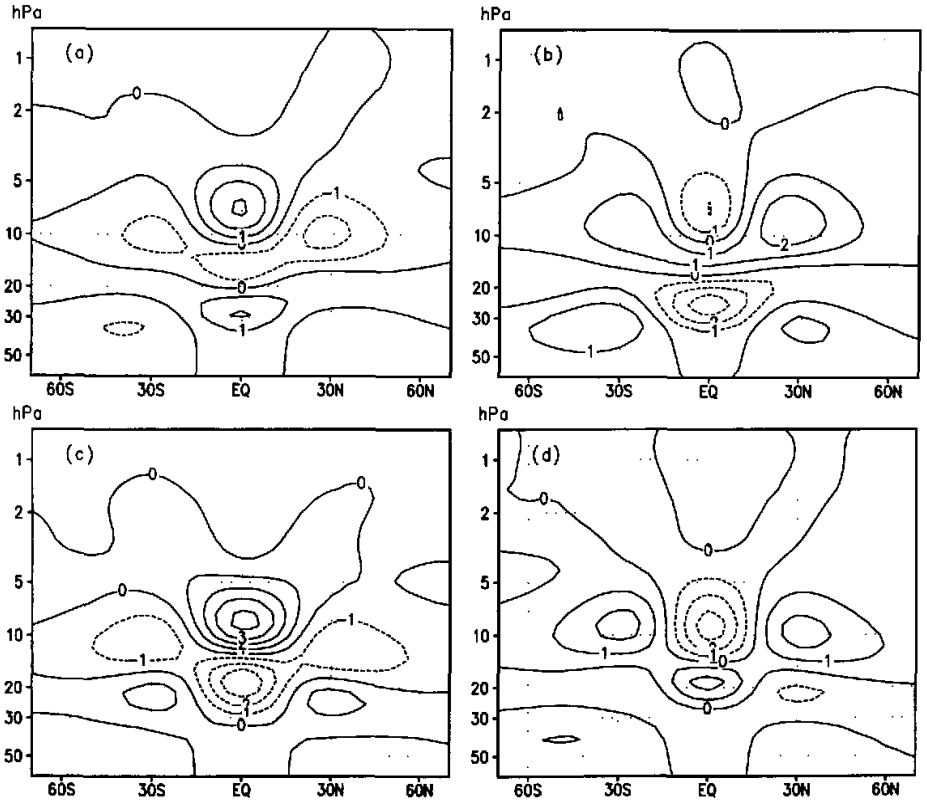

Fig. 6. As in Fig. 5 except (a) for JJA in westerly phase, (b) for JJA in easterly phase, (c) for SON in westerly phase, and (d) for SON in easterly phase.

(Fig. 8a), when the easterly began and increased in intensity, because the induced cells continued moving down, the cells which were originally above just replaced the middle cells and these, in turn, just replaced the cells below. At that time, the locations of the three pairs of cells were almost the same as in October of the first model year, except the directions of the cells were reversed. With the changes in the wind phase, the locations of the induced circulation changed continuously in cycles. It should be noted that the locations of the cells were not dependent on the seasons but depended on the stage of the westerly and easterly. When the simulations came to January of the fourth model year and May of the sixth model year, the location and direction of the three pairs of cells were almost the same as those in October of the first model year, which was the stage of westerly strength. Similarly, when the simulation reached February of the fifth model year, in the stage of easterly strength, the location and direction of the three pairs of cells were almost the same as those in October of the second model year (figures omitted).

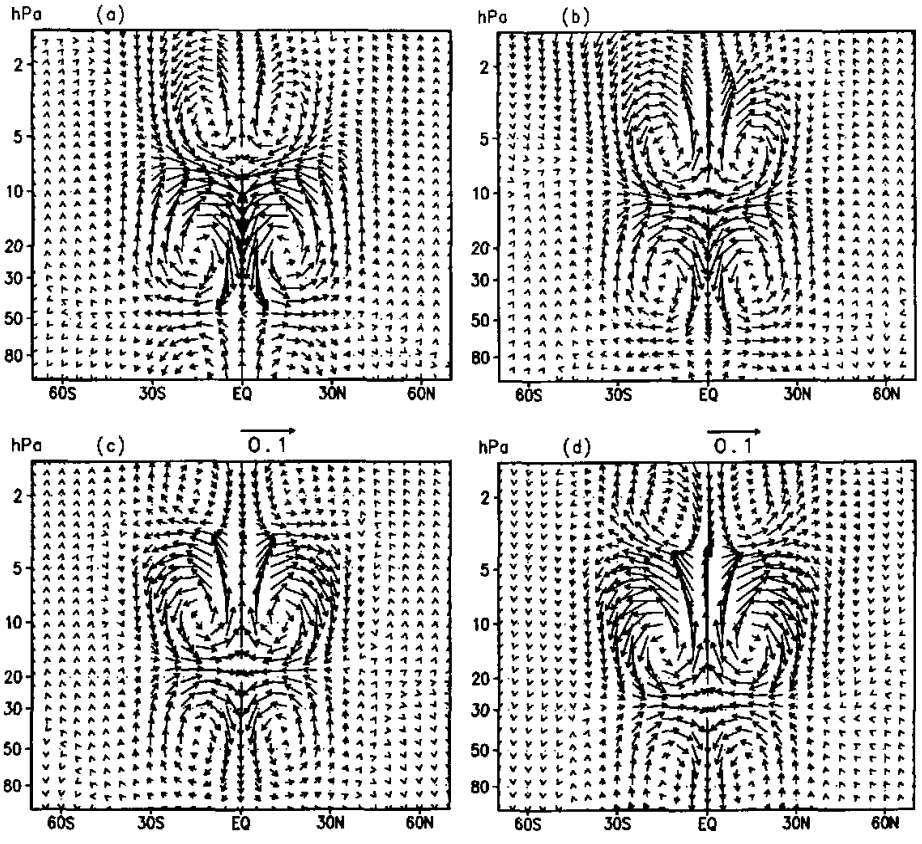

Fig. 7. Simulated residual circulation induced by wind QBO in the westerly phase. (a) For October, first model year; (b) for January, second model year; (c) for April, second model year; and (d) for July, second model year.

In order to discuss how the wind QBO leads to displacement of the high region of ozone mixing ratio in the stratosphere and the change of vertical distribution of ozone density, the ozone partial pressure simulated without wind QBO has been superimposed on the induced meridional circulation in Fig. 9. The solid lines in the figure represent the distribution of ozone partial pressure without wind QBO forcing. We can see from Figs. 9a and 9b that in the case without wind QBO, the center of high ozone density is located to the north of the equator in July. This is because solar radiation is stronger in the Northern Hemisphere and the maximum ratio of photochemical ozone generation occurs between the equator and the Tropics of Cancer in this season. With this kind of disposition of the residual circulation and the center of high ozone density, in the westerly phase in July (as in Fig. 9a) the air with high-density ozone at 18 hPa and nearby over 15°–20°N was transported toward the equator, so that ozone density over the region near the equator increased. Moreover, the air with low-density

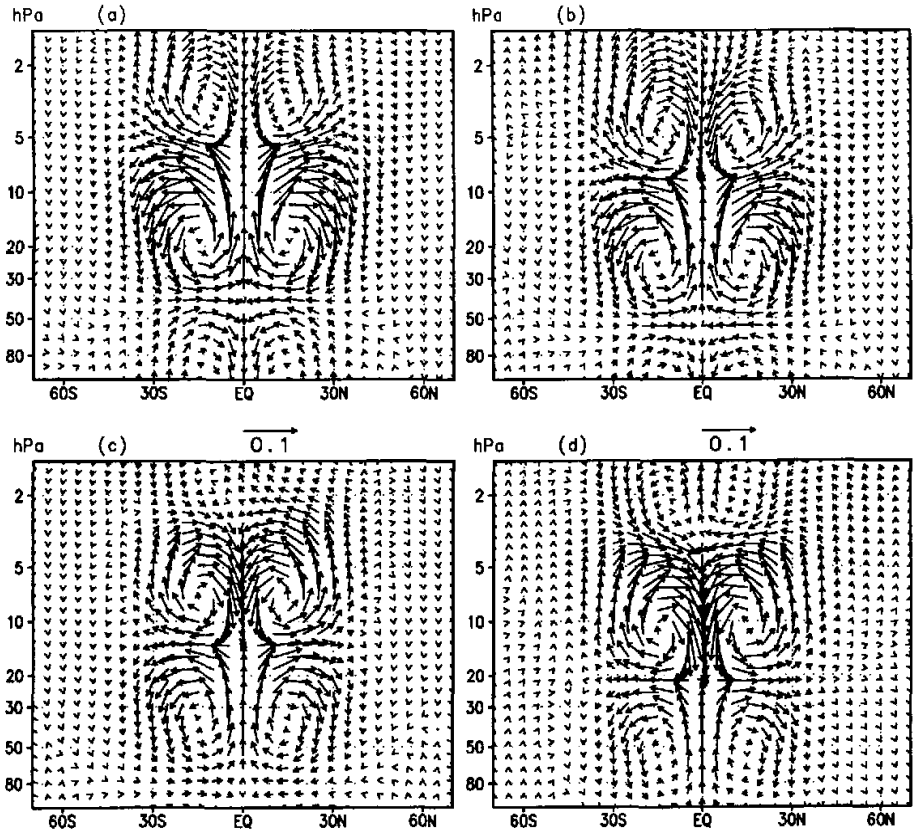

Fig. 8. Simulated residual circulation induced by wind QBO in easterly phase, (a) For October, second model year, (b) for January, third model year, (c) for April, third model year, and (d) for July, third model year.

ozone in the middle stratosphere over the extratropics was transported downward, which led to the decrease of ozone density near 18 hPa over the extratropics. The consequence was the equator-ward movement of the center of high ozone density in July during the westerly phase. In the easterly phase, because of the reversed direction of residual circulation, ozone was transported in the opposite direction leading to the displayment of the center of high ozone density toward the extratropics (as shown in Fig. 9b). The transportation of ozone by the induced circulation in April are shown in Figs. 9c and 9d. In this month, the simulated center of higher ozone density without wind QBO was located mainly over the equator. In the westerly phase with the effect of the induced cells shown in Fig. 9c, the ascending flow over the equator near the center of high ozone density transported the air with rich ozone upward, which led to the increase of ozone density on the top of the high center. Therefore the region of high ozone density extended upward. It was opposite in the easterly phase. The air with low-density ozone above the high center moved down, which made the ozone density

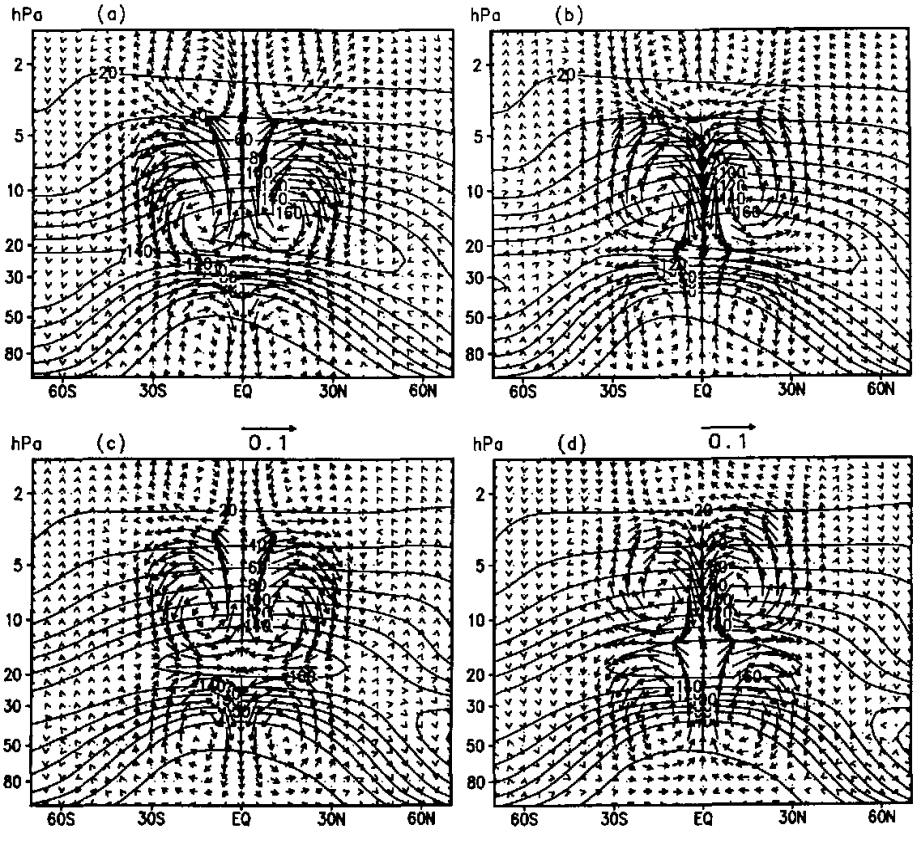

Fig. 9. Simulated wind QBO–induced residual circulation (vectors) and ozone partial pressure without wind QBO forcing (contours, units:in 10^{-6} hPa). (a) Westerly phase, July, (b) easterly phase, July, (c) westerly phase, April, and (d) easterly phase, April.

decrease on top of the center of high ozone density over the tropics. Therefore the high center became thinner and spread to the extratropics. The situation in January and October can be explained in the same way. Therefore, it can be proved that the QBO of the center of high ozone density is largely due to zonal wind QBO–induced residual cells in the middle atmosphere. As mentioned above, the oscillation of the center of high ozone density in north–south direction and the change of its thickness are important reasons for the QBO of column ozone over the tropics and extratropics. Although the residual circulation induced by the zonal wind QBO is symmetric about the equator, the location of the high center of ozone density changes with seasons and is not hemispherically symmetric. It swings in the north–south direction by the effect of wind QBO, so that the transportation of ozone by the induced circulation in various latitudes is not the same, which makes the ozone QBO hemispherically asymmetric. This shows that the wind QBO–induced residual circulation in the middle stratosphere (near 25–

5 hPa) plays an important role in the generation of ozone QBO over the tropics and extratropics as well as in the hemispheric asymmetry of ozone QBO.

From the disposition of the simulated residual circulation and the center of higher ozone density we can also find the reason the QBO phase of ozone density changes many times vertically. As mentioned above, the induced circulation in the stratosphere includes three pairs of cells vertically. We can see from Fig. 9a and 9b that the vertical velocities in 25–5 hPa are opposite from those above 4 hPa and below 25 hPa. In the westerly phase and over the equator, the induced upward flow in 14–5 hPa transports the air with rich ozone upward and leads to an increase in ozone density in the 12–3 hPa layer while the induced upward flow in 22–18 hPa transports the air with lower ozone density upward and reduces the ozone density near the 20 hPa level. Below 25 hPa over the equator, the induced downward motion transports the air with higher ozone density to a lower level, so that the ozone density increases below 25 hPa. At the same time, the induced downward flow above 3 hPa transports the air with lower ozone density downward. So there is a region with ozone density decrease above 3 hPa. As a result, the signal of ozone density departure changes many times vertically. The transports in various levels in the easterly phase are reversed, which will not be given explicitly here. The situation in other seasons can be discussed in the same way, except that the location of the signal reversals and the strength of the variation of ozone density are somewhat different. This is because the downward motion of the induced residual cells make the disposition of the three pairs of induced cells and the center of high ozone density somewhat different in various seasons. Thus we can explain the structure of ozone QBO shown in Figs. 5 and 6 which also agrees well with the result from HALOE data analysis.

The three pairs of induced residual cells are mentioned on many occasions in this paper, and the cells in the middle stratosphere (in 25–5 hPa) are emphasized. This is because in previous studies, only the induced circulation in the lower stratosphere was taken into account to explain the generation of ozone QBO (Ling and London 1986; Andrews et al. 1987; Gray and Pyle 1989). It was suggested that in the easterly shear zone the induced upward motion in the tropics transported ozone–poor air into the lower stratosphere and it reduced the column ozone there. In the westerly shear zone, it is in the opposite way that the induced downward motion results in a positive total ozone perturbation. However, we can see from our simulation that although the changes of vertical motion in the lower stratosphere play a certain role for the generation of ozone QBO, the effects of the induced residual circulation in the middle stratosphere are also important. This is because on one hand, the induced residual circulation in the middle stratosphere has quite a strong vertical and meridional flow at the altitude where there is maximum ozone density, so it is advantageous for ozone transport. On the other hand, interannual variation of meridional ozone transport to the extratropics is an important reason not only for the generation of ozone QBO in the tropics and extratropics but also for their phase reversal. From Fig. 6 we can see that the changes of ozone density in the middle stratosphere over the extratropics are more clear than those in the lower stratosphere. Thus it is not enough to explain the generation of ozone QBO using only wind QBO–induced variation of vertical motion in the lower stratosphere.

6. Conclusions

Based on the analysis of HALOE observational data from 1992–2000 and a numerical experiment using the NCAR interactive chemical, dynamical, and radiative two–dimensional model, we draw the following conclusions.

1) The vertical distribution of ozone mixing ratio in the stratosphere clearly shows a seasonal variation. In MAM and SON, the high center of ozone mixing ratio was nearly over the equator, and in JJA it moved to the Northern Hemisphere, and in DJF it moved to the Southern Hemisphere, which corresponds to the seasonal variation of the intensity of solar radiation in various latitudes.

2) The interannual variation of stratospheric ozone mixing ratio shows in two aspects. First, the zones of high ozone density around the 10 hPa level over low latitudes diminished year by year during 1992–1995, changed little in 1996 and 1998, and were enhanced somewhat in 1999 and 2000. Second, the center of high ozone density in the stratosphere moved meridionally and vertically with a quasi-biennial period, and the oscillation of the high center of ozone density in various seasons is different, which largely correlates with zonal wind QBO. The simulations agree well with the observations.

3) In the tropical regions, the phase of QBO for ozone density changed many times with height. The phase of ozone QBO at the 50–20 hPa level is opposite to that near 13 hPa, while alike to that near 5 hPa. At about the 2–3 hPa level, the phase changed again. This is shown by numerical experiment.

4) The model results show that the induced meridional circulation by wind QBO (residual circulation) consists of three pairs of cells vertically aligned in the stratosphere. They are symmetric about the equator. The ozone transport in different altitudes and latitudes by the induced residual circulation is one of the important causes of the ozone QBO. In particular, the cells of residual circulation in the middle stratosphere (25–5 hPa) plays an important role in producing the ozone QBO.

5) Since the intensity of solar radiation reaching different latitudes varies seasonally, the region of the maximum photochemical production rate for ozone also changes with the seasons. Therefore the location of the high center of ozone density changes with the seasons and it is not hemispherically symmetric. In particular, it swings in a north–south direction according to the effect of the wind QBO. So, although the induced meridional circulation is symmetric about the equator, the transportation of the ozone by the induced circulation in various latitudes is not the same, which makes the ozone QBO hemispherically asymmetric.

Acknowledgments. The authors would like to express their thanks to the HALOE Science and Engineering teams who have worked so hard to provide an excellent data set and to NCAR for providing the NCAR interactive chemical, dynamical, and radiative two-dimensional model. And this work is supported by the Open Laboratory for Middle Atmosphere and Global Environment Observation, IAP / CAS).

REFERENCES

Andrews, D. G., J. R. Holton, and C. B. Leovy, 1987: *Middle Atmospheric Dynamics*, Academic Press, 489pp.

Chen Wen, and Huang Ronghui, 1996: The numerical study of seasonal and interannual variabilities of ozone due to planetary wave transport in the middle atmosphere. *Chinese Journal of Atmospheric Sciences*, **20**(3), 513–523 (in Chinese).

Dunkerton, and J. Timothy, 2001: Quasi-biennial and subbiennal variations of stratospheric trace constituents derived from HALOE observations. *J. Atmos. Sci.*, **58**, 7–25.

Funk, J. P., and G. L. Garnham, 1962: Australian ozone observations and a suggested 24 month Cycle. *Tellus*, **14**, 378–382.

Gray, L. J., and J. A. Pyle, 1989: A Two-dimensional model of the quasi-biennial oscillation of ozone. *J. Atmos. Sci.*, **46**, 203–220.

Gray, L. J., and S. Ruth, 1993: The modeled latitudinal distribution of the ozone quasi-biennial oscillation using

observed equatorial winds. *J. Atmos. Sci.*, **50**, 1033–1046.

Hasebe, F., 1983: Interannual variations of global ozone revealed from Nimbus 4 BUV and ground-based observations. *J. Geophys. Res.*, **88**, 6819–6834.

Hasebe, F., 1994: Quasi-biennial oscillation of ozone and diabatic circulation in the equatorial stratosphere. *J. Atmos. Sci.*, **51**, 729–745.

Hess, P. G., and D. O'Sullivian, 1995: A three-dimensional modeling study of the extratropical quasi-biennial oscillation in ozone. *J. Atmos. Sci.*, **52**, 1539–1554.

Huang, T., S. Walters, G. Brasseur, D. Huaglustaine, W. Wu, S. Chabrillat, X. Tie, C. Granier, A. Smith, S. Madronich, and G. Kockarts, 1997: Description of SOCRATES, A chemical, dynamical, radiative 2-D model, Technical Report, NCAR, Boulder, Colorado.

Jones, D. B. A., H. R. Schneider, and M. B. McElroy, 1998: Effects of the quasi-biennial oscillation on the zonally averaged transport of tracers. *J. Geophys. Res.*, **103**, 11235–11249.

Ling, X., and J. London, 1986: The quasi-biennial oscillation of ozone in the tropical middle stratosphere: A one-dimensional model. *J. Atmos. Sci.*, **43**, 3122–3137.

Li Yanlong, Chen Zhaoyang, and Li Shuangke, 1997: Quasi-biennial oscillation of atmospheric ozone amount. *Journal of Gansu University of Technology*, **23**(4), 96–101.

Ramanathan, K. R., 1963: Bi-annual variation of atmospheric ozone over the tropics. *Quart. J. Roy. Meteor. Soc.*, **89**, 540–542.

Yang, H., and K. K. Tung, 1995: On the phase propagation of extratropical ozone quasi-biennial oscillation in observational data. *J. Geophys. Res.*, **100**, 9091–9100.

Zhang Hong, Chen Yuejuan, and Wu Beiying, 2000: Impact of quasi-biennial oscillation on the distribution of the trace gases in the stratosphere. *Chinese Journal of Atmospheric Sciences*, **24**(1), 103–110 (in Chinese).

热带平流层臭氧准两年周期振荡的特征及数值模拟

陈月娟　郑　彬　张　弘

摘　要

利用 HALOE 的观测资料，对热带地区平流层臭氧垂直分布的年际变化及其准两年周期振荡(QBO)进行研究，并同赤道上空平均的纬向风场的准两年周期振荡进行对比，并利用 NCAR 的二维模式就风场的 QBO 对平流层臭氧分布和变化的影响机理进行了模拟研究。资料分析结果表明，平流层臭氧浓度高值区的位置在南北方向上和垂直方向上的变化有明显的准两年周期，臭氧浓度高值中心的南北移动和上下移动又引起局地臭氧总量的周期性变化和准两年周期振荡南北半球不对称。而臭氧浓度中心位置的准两年周期变化与赤道上空平均纬向风的准两年周期振荡密切相关。资料分析还表明，赤道上空平流层中臭氧浓度 QBO 的位相随高度变化多次。模拟试验表明，纬向风 QBO 引起垂直经圈环流的变化，在平流层有三对余差环流圈，它们对 O_3 在不同纬度和高度的输送是引起 O_3 准两年周期振荡的重要动力原因。其中，余差环流在平流层中层(25–35 km)的环流圈起着重要的作用。

关键词：臭氧 QBO, HALOE 资料, NCAR 模式, 数值模拟